Palpation Tomography – A New Technique for Modulus Estimation in Elastography

E. E. Konofagou[1] and T. P. Harrigan[2]

[1]Department of Biomedical Engineering, Columbia University, New York, NY, USA; [2]Exponent Failure Analysis Associates, Natick, MA, USA

Abstract - In Elastography, strain estimation has been shown to be far more reliable compared to the elastic properties obtained using reconstruction techniques. In this study, to make the method less sensitive to noise in the experimental data and inspired by the clinical practice of palpation (i.e., the use of sequential finger loading), we investigated the effect of using several different smaller quasi-static load cases (instead of a one-time load on the whole boundary), with the error indicator taken as the sum of the errors from each load case. This increased the ratio of measurements to the fitted parameters, which made the method less sensitive to random errors. To demonstrate this effect, we calculated displacements from a two-dimensional, quadrilateral, plane-strain, finite-element model of a 40-by-40 mm region containing a cylindrical inclusion (7 mm in diameter) three-times stiffer than the background. The ratio of nodal pressures was chosen to produce approximately 0.75% strain. Known amounts of random displacement errors were then added at a signal-to-noise ratio varying from 60 dB to 20 dB. Elastic modulus reconstructions using the noisy displacement results from a single, total-boundary, pressure load (as is typically applied in elastography) [1] were compared to reconstructions using data from nine smaller-width loading cases, and the reconstructed modulus distributions were compared to the original model parameters. It was found that in the cases of 60 dB and 40 dB the multiple loading cases resulted in noise reduction in the modulus reconstruction by at least a two-fold compared to the single-loading case, at the expense of a 'shadowing' effect (i.e., erroneous modulus estimates) underneath the inclusion that could be eliminated by using larger loading areas for the individual loading cases. Finally, at 20 dB both the large single-load and combined, smaller five-load cases failed to accurately reconstruct the modulus of the inclusion; depicting thus a fundamental limit on the reconstruction method.

I. INTRODUCTION

Material property estimation from motion information has been an objective from the initial development of the technique [2]. The essentials of the technique are based on an imaging procedure usually ultrasound or MRI) in which reflections or tagged volumes of material are tracked within an image during an imposed or naturally-occurring deformation. By tracking small inhomogeneities within the tissue (such as speckle in an ultrasound image, or tagged regions in an MRI image) a deformation field within the region being analyzed can be measured [3]. This allows an estimate of local strain to be made, based on a numerical derivative of deformation with position, and the interpretation of these strain fields in tissues is usually made to find areas where the local material modulus is high, which often indicates a pathologic state [4]. Many procedures currently used for the estimation of material properties involve intermediate calculation of strain data [5,6], often using shear-wave propagation to estimate local material properties [7,8]. Kallel et al [9] developed an elastic modulus estimation technique by minimizing the sum of squared errors between a measured set of displacements and a set of displacements that was from a numerical elasticity model. The technique is numerically difficult, involving the inversion of a large matrix, which is ill-conditioned numerically. Our technique is based on a similar minimization algorithm, but the resulting numerical algorithm is simpler and may thus be more robust [1]. In this case, we apply the reconstruction technique previously described in combination with multiple loading. Borrowing from the practice of palpation and the use of sequential independent loading for the detection of an underlying lesion, we verify whether the multiple loading case eliminates random noise that may corrupt the modulus reconstruction estimate.

II. THEORY

The cost function we used in prior work [1] is based on comparing the actual displacements to the displacements in a finite element mesh using a provisional elastic modulus distribution. The difference in displacement is used in an energy expression as follows:

$$\Psi = (v_i - u_i)K_{ij}(v_j - u_j) \qquad (1)$$

with v_i the displacements of nodes computed using a finite element model, u_i the measured displacements at the positions corresponding to the nodes in the finite element mesh, and K_{ij} the stiffness matrix in from the finite element mesh. The indices i and j indicate the degrees of freedom within the finite element model. Physically, $(v_i\text{-}u_i)$ corresponds to the error between the predicted displacements in the finite element model and the measured displacements.

The stiffness matrix K_{ij} is the sum of the stiffness matrices for each of the elements. The elastic modulus in these individual element is initially taken as uniform, and the distribution of elastic modulus is progressively updated. Minimizing the cost function corresponds to minimizing the energy stored by the displacement errors. Since, in any finite element model of elastic bodies, the stiffness matrix K_{ij} is positive-definite, the error function will be positive, and will only be negative when the vector $(v_i\text{-}u_i)$ is identically zero.

If this method is considered as a fitting operation, then the number of adjustable parameters is equal to the number of elements, and the number of experimental measurements used to predict these parameters is equal to the number of displacements. This means that the number of adjustable parameters is slightly less than half the number of measurements, which makes the elastic modulus distribution very noise-sensitive. In order to get a larger measurement-to-parameter ratio, we use multiple load cases. That is we use

$$\Psi = \sum_p \left(v_i^p - u_i^p\right)K_{ij}\left(v_j^p - u_j^p\right) \qquad (1)'$$

with p the load case number. That is, v_i^p is the computed displacement number *"i"* for load case *"p"*. This allows an averaging out of random noise and it also makes the individual displacement fields more complex, possibly uncovering more detail in the modulus distribution. The resulting rate equation is

$$\frac{\partial \phi_e}{\partial t} = \sum_p \frac{1}{\phi_e}\left[v_e^p\left(\phi_e K_{ij}^e\right)v_e^p - u_e^p\left(\phi_e K_{ij}^e\right)u_e^p\right] \qquad (2)'$$

which is a series of differences between the elastic energy stored in individual finite elements with ϕ_e the indicator variable for element e.

III. METHODS

In order to reduce the noise on the modulus estimate, one example of multiple loading was considered. The number of vertical loads was nine (Fig. 1) instead of the typical loading of a single load. The different loads did not overlap. The sides of the model were unconstrained, and the bottom of the model in Fig. 1 was constrained so that vertical motion was prevented but horizontal motion was allowed except at the middle node. The displacement distribution u_i for the feasibility study was taken from a linear elastic calculation using the target elastic modulus distribution. The number of nodes and quadrilateral elements was equal to 2501 and 4800, respectively.

Since the finite element formulation is static and linear, the units and lengths used for the physical variables scale according to well-known characteristics. The region considered was 40 mm by 40 mm with an 8-mm inclusion. The outer part of the finite element model has an elastic modulus of 100 MPa, and the simulated inclusion has an elastic modulus of 300 MPa. The applied strain was equal to 1% in each case.

Using scaling arguments, these displacements also correspond to the case where the outer material has an elastic modulus of 100 kPa, the inclusion has an elastic modulus of 300 kPa, and the applied loading simulates a uniform pressure of 0.4 kPa. The Poisson ratio for both the inclusion and the surrounding material was taken as 0.4 during the calculations of the target displacement field u_i. Simulated RF signals were generated for each loading case and different amounts of random noise were added on the signals prior to the estimation. The sonographic SNR acquired the following values: 10, 20, 40 and 60 dB. For each loading and SNR case the axial and lateral, displacement and strain were estimated using previously described techniques [2] and a 3 mm window with a 60% overlap. Finally, the 2D displacement information was fed into the reconstruction algorithm for the calculation of the modulus.

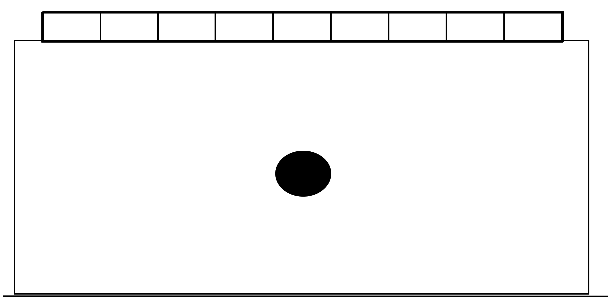

Figure 1: An example of palpation tomography using individual loading (in this case, nine loads).

IV. RESULTS

Figures 2 and 3 depict the axial and lateral displacement images for the nine-load case, respectively. The axial displacement was estimated at all sonographic SNR levels at a good SNR. However, the lateral displacement had a very poor SNR at 10 dB sonographic SNR. At 20 dB, the quality is improved but only at 40 dB is it as good as that of the axial displacement estimation. The same hold for the single loading case (Fig. 4). Therefore, only the cases of 20-60 dB were considered for the reconstruction of the modulus (Fig. 5). As shown in Fig. 5, using nine loading cases diminished the noise in the predicted elastic modulus distribution substantially. In the 20 dB case, however, the averaging method did not result in a recognizable distribution of modulus; possibly due to the poorer lateral displacement SNR.

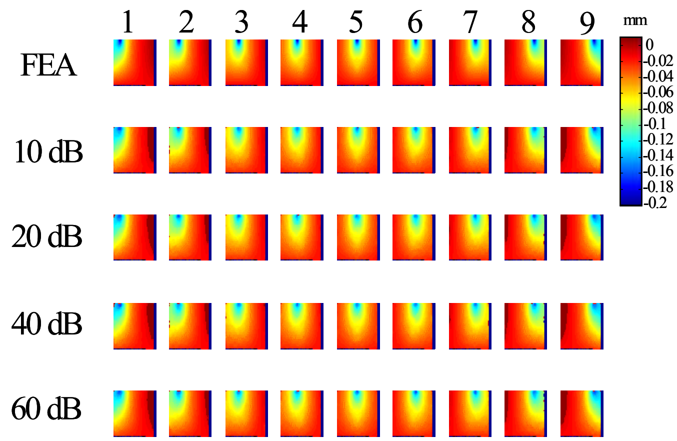

Figure 2: Axial displacement images for each loading case and sonographic SNR.

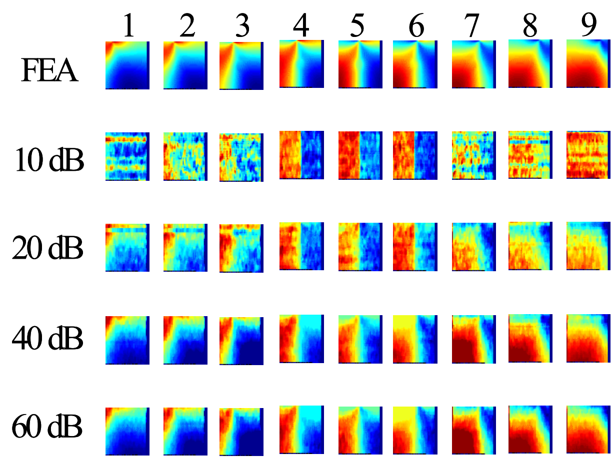

Figure 3: Lateral displacement images for each loading case and sonographic SNR calculated from the images in Fig. 4. The colorscale varies: in images 1-3 the strain ranges from 0 to 0.08, in 4-6 from –0.01 to 0.04 and in 7-9 from –0.07 to 0.

V. DISCUSSION

We showed that multiple loading using nine loading cases can significantly increase the quality of the reconstruction technique previously described. Both axial and lateral displacements were obtained at good SNR at noise levels higher than 20 dB. The lower noise achieved also induced an artifact in the final modulus image appearing as a shadowing artifact behind the inclusion. This may be due to the type of load used, the size and the overlap between the different loads. Future studies will include the study of different number, size and overlap of loads as well as identification of the artifact origin.

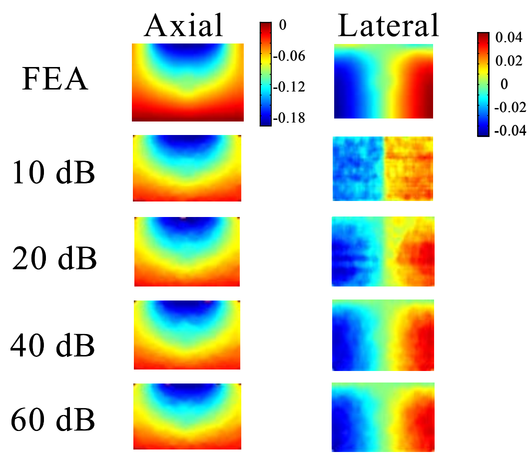

Figure 4: Axial and lateral displacement images in the case of the single loading case (i.e., using all nine loads in Fig. 1 together).

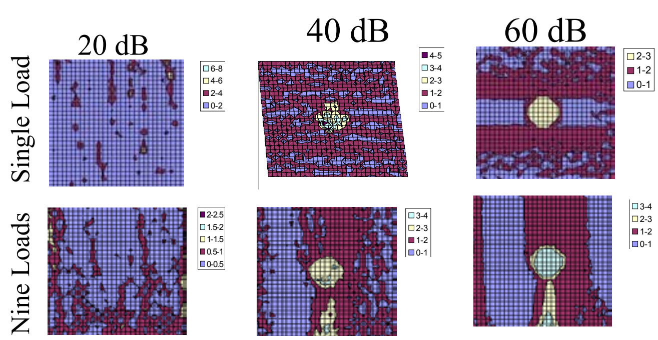

Figure 5: Reconstructed modulus images for each loading example at different sonographic SNR lev els.

VI. ACKNOWLEDGMENT

This study was supported by a fellowship grant from the American Society of Echocadiography.

VII. REFERENCES

[1] Harrigan T. and Konofagou E.E., Harrigan T and Solomon, S, J. Biomech., 2003 (in press).

[2] Ophir, J., S. K. Alam, et al., Elastography: ultrasonic estimation and imaging of the elastic properties of tissues, Proc Inst Mech Eng [H] 213(3): 203-33, 1999.

[3] Kallel, F., J. Ophir, et al. ,Elastographic imaging of low-contrast elastic modulus distributions in tissue, Ultrasound Med Biol 24(3): 409-25, 1998.

[4] Plewes, D. B., J. Bishop, et al. (2000). "Visualization and quantification of breast cancer biomechanical properties with magnetic resonance elastography." Phys Med Biol 45(6): 1591-610.

[5] Skovoroda, A. R., Emelianov, S. Y., O'Donnel, M., Tissue elasticity reconstruction based on ultrasonic displacement and strain images, IEEE Trans Ultrason. Ferroel. Freq. Cont., 42, 747-765, 1995.

[6] Sumi, C., Suzuki, A., Nakayama, K., "Estimation of shear modulus distribution in soft tissue from strain distribution", IEEE Trans. Biomed, Eng., 193-202, 1995.

[7] Sandrin, L., M. Tanter, et al., Shear modulus imaging with 2-D transient elastography, IEEE Trans Ultrason Ferroelectr Freq Control 49(4): 426-35, 2002.

[8] Tanter, M., J. Bercoff, et al., Ultrafast compound imaging for 2-D motion vector estimation: application to transient elastography, IEEE Trans Ultrason. Ferroel. Freq Control 49(10): 1363-74, 2002.

[9] Kallel, F., Bertrand, M., Ophir, J., Advances in tissue elasticity reconstruction using linear perturbation method, Acoustical Imaging, J. P. Jones (ed), PLenum Press, New York, NY, 22, 267-277,1996.